An experimental and numerical study on deposition of bioaerosols in a scaled chamber

L.T. Wong,[1] A.C.K. Lai,[2] W.Y. Chan[1] and K.W. Mui[1]*

[1]Department of Building Services Engineering,

The Hong Kong Polytechnic University, Hong Kong, China.

[2]Department of Building & Construction,

City University of Hong Kong, Tat Chee Avenue, Kowloon, Hong Kong, China

*Corresponding Author: K.W. Mui

Email: behorace@polyu.edu.hk

Tel: (852) 2766 5835

Fax: (852) 2765 7198

Abstract

This work presents an experimental facility designed and built with the objective of understanding the deposition of bioaerosols in indoor environments. Multiple depositions of two microorganisms *Staphylococcus* and *Micrococcus* inside a test chamber were investigated under two air mixing conditions. Airflow rate was demonstrated to have an influence on the concentration homogeneity. An increased proportion of particle deposition was found in the floor section near the chamber wall opposite to the air inlet when air mixing was not enhanced by the mixing fans. Both the experimental results and Eulerian-Lagrangian computations revealed that a small mixing fan inside the chamber prompted very effective mixing while non-homogeneity was observed even at a very high ventilation rate. The results showed that both ventilation rate and mixing conditions in the ventilated chamber have influence on the bioaerosol dispersion and deposition.

1. INTRODUCTION

Hong Kong is located in the subtropical zone and its climate is classified as 'Humid Subtropical'. Most buildings in Hong Kong are equipped with air-conditioning and mechanical ventilation systems for acceptable indoor environments (Lai et al. 2009; Wong et al. 2006). To maintain the desired distributions of air temperature, relative humidity, air speed and age of air, a properly designed air diffusion system is a must.

In a ventilated enclosure, the location and air supply direction of an air inlet dictate airflow patterns as well as velocity fluctuations and thus have significant effects on the diffusion performance (Fanger et al. 1988; Chow and Wong 1994; 1998a). According to a survey study on typical air diffusion systems for air-conditioned and mechanically ventilated offices in Hong Kong, 76% of the air inlet devices mounted in or near the ceiling discharged air horizontally while the rest projected air vertically down (Chow and Wong 1998b). The ranges of air temperature, relative humidity and air speed recorded at the air inlets were from 15 to 27.6 °C, 48 to 82% and 0.15 to 3.05 ms^{-1} respectively. Except for a few extreme cases (i.e. small offices in which problems of providing low ventilation rate were raised), the ventilation rates of the surveyed offices ranged between 2 and 40 h^{-1}. Reportedly, ventilation effectiveness can be characterized by the age of air (Sandberg and Sjoberg 1983).

Since the outbreak of severe acute respiratory syndrome (SARS) in 2003 (swine flu is yet another concern currently), research interests in the control of airborne microorganisms indoors have been mounting (Chao et al. 2008; Mui et. al. 2009). Studies show that airborne transmission of infectious agents in an indoor space is related to ventilation airflow patterns (Wan and Chao 2007; Li et al. 2007). These agents are usually carried in by the building occupants or via ventilation air supply (Otten and Burge 1999). The most abundant indoor (cultivable) airborne

bacteria are gram-positive cocci, such as *Micrococcus* and *Staphylococcus* which represented 38% of the composition of airborne bacteria discovered in a survey of 100 buildings in USA while equaled 100% of what was found inside the sampled dwellings in a Poland study (Górny and Dutkiewicz 2002; Tsai and Macher 2005). It is noted that culture-based techniques can identify less than 1% of the indoor microbial community and instead indentify the species that are easily cultured (Toivola et al. 2002). *Micrococcus* spp. and *Staphylococcus* spp. are common indoor inhabitants shed from human skin surfaces and easy to be identified in culture-based techniques. When *Staphylococcus aureus* is facultative anaerobic, *Micrococcus luteus* is strictly aerobic. Both of them may occur singly, in pairs, tetrads or irregular clusters. It is known that *Staphylococcus aureus* is a major multidrug-resistant pathogen that is the most prevalent cause of hospital- and community-acquired bloodstream, skin, soft tissue, and lower respiratory infections (Gandara et al. 2006).

An understanding of the role of ventilation in bioaerosol dispersion and deposition is essential in assessing bacteria exposure and preventing airborne infection indoors (Lai 2002; Li et al. 2007; Wan and Chao 2007; Gao and Niu 2007; Zhao et al. 2005; Nazaroff 2004). A drift-flux model for particle distribution and deposition in indoor environments was applied for investigation of spatial and temporal particle concentration in enclosures even the well-mixed assumption cannot hold for coarse particles (Lai and Cheng 2007). Kanaani et al. (2008a) investigated the deposition rates of airborne fungi (*Aspergillus niger* and *Penicillium* sp.) in a chamber installed with ceiling-mounted air diffusers operating at a ventilation rate up to 2.5 h^{-1} and reported that the deposition rates of the test fungal spores and other aerosols of comparable size were similar, especially at very low ventilation rates. Their results also showed increasing deposition rates with increasing ventilation rates.

Although particle deposition of biological and non-biological aerosols have been studied, computational fluid dynamics (CFD) predictions of bioaerosol distribution patterns in a specific type of air distribution system over a wide range of ventilation rates have never been detailed. The key objectives of this study are: (1) to design an experimental setup for measuring the spatial deposition of two ubiquitous bacteria, namely *Staphylococcus aureus* and *Micrococcus luteus*, in a common type of air distribution system; (2) to delve into the influence of various airflow rates and mixing conditions on the spatial deposition; and (3) to compare the experimental results with CFD prediction.

2. METHODOLOGY

2.1 Experiments

Transport, distribution and deposition patterns of bioaerosols were measured inside a 70L ventilated chamber of size 0.650 m (L) × 0.380 m (W) × 0.284 m (H) placed in a Class II biological safety cabinet. The chamber was constructed of tempered glasses. Openings on the chamber surfaces allowed tests to be conducted under some ventilation arrangements. To determine the chamber leakage rate, concentration decay tests with all openings covered were done repeatedly over a two-hour period at an average initial carbon dioxide (CO_2) concentration of 4,000 ppm. The leakage rate found was 2.4×10^{-3} min^{-1} and the chamber was categorized as a Class 2 containment enclosure which was suitable for the subsequent experiments (ISO 1994).

Figure 1 shows the experimental setup. Compressed air, first filtered through an air filtration system ‘a’ (Model 3074B, TSI) for moisture and impurities removal, entered the cabinet via two air paths f_1 and f_2, and then passed into air path f_3. f_1 was for the adjustment of

aerosol concentration by volume while f_2 was connected to a 6-jet collision nebulizer 'c' (BGI Inc. Waltham, MA) for bioaerosol generation. The volume flow rates in f_1 (ranged from 0 to 20 L min^{-1}), f_2 (fixed at 15 L min^{-1}) and f_3 could be conditioned and were gauged by the flow meters 'b_1', 'b_2' and 'b_3' respectively. Moisture was removed again in f_3 via a diffusion dryer 'd' (Model 3062, TSI). The processed air was finally supplied to the chamber through a high sidewall inlet 'e_1' and exhausted through an outlet 'e_2' aligned on the opposite chamber wall. This composition was one of the common ventilation configurations; the isothermal air diffusion performance in a room of similar layout had been investigated in a previous study (Chow and Wong 1998c). Both the inlet and outlet were circular with a diameter of 0.016 m. Two identical small muffin fans 'g_1' and 'g_2' were installed in the chamber to enhance air mixing.

<< Figure 1: Experimental setup >>

Staphylococcus aureus (American Type Culture Collection, ATCC 6538; cell diameter 0.7-1.0 μm) and *Micrococcus luteus* (ATCC 4698; cell diameter 0.9-1.8 μm) were used as the reference bacteria in this study (Holt et al. 1994; Stanley 1989). Their sample cells were considered spherical with an average diameter of 1 μm as illustrated in Figure 2. Initially, the bacterial cultures were inoculated on Tryptone Soya Agar (TSA, Oxoid) and incubated at 30°C for 24 hours. After that, a single colony was picked from the TSA, inoculated into 10 ml Tryptone Soya Broth (TSB, Oxoid) and incubated at 30°C under aerobic conditions for another 24 hours. A method of harvesting aerosolized bacteria followed (Kanaani et al. 2008b). For aerosolization, a 50 ml bacterial suspension was stored in the collision nebulizer 'c' (Figure 1). Measurements were started within an hour to keep the bacterial viability. To decide the amount of viable cells, serial dilutions were made in sterilized Ringer's solution, and a 0.1 ml sample of the diluted suspension was spread on triplicate TSA plates and incubated at 30°C for 24 hours

for counting. Prior to all deposition distribution tests, 0.1 m^3 air samples were collected by the Biostage Single-stage Viable Cascade Impactors placed in the chamber to determine the original bioaerosol concentrations. Throughout the operating period, bioaerosol concentrations were measured to ensure a steady state inside the chamber.

<< Figure 2: Reference bacteria >>

A total of 28 TSA plates organized in an array of 7 columns by 4 rows were placed on the chamber floor to record the bioaerosol deposition patterns. The arrangement is depicted in Figure 1. For each deposition distribution test, bioaerosols were supplied into the chamber through inlet 'e_1' for 60 minutes in the form of an air jet under isothermal conditions. The plates were then collected and incubated at 30°C for 24 hours before the colonies on each plate were counted. Repeated measurements were conducted at inlet velocities 0.17 ms^{-1}, 0.58 ms^{-1}, 1.0 ms^{-1}, 1.4 ms^{-1} and 1.8 ms^{-1} with respect to ventilation rates 1.7 h^{-1}, 6 h^{-1}, 10.3 h^{-1}, 14.5 h^{-1} and 18.8 h^{-1}. The selected ventilation rates between 1 to 19 h^{-1} are typical range for ventilated enclosures. This study concentrates mainly on the deposition. It has been shown that in a similar sized ventilated chamber, majority of the particles of size 1 μm were transported outside the chamber (Lai and Chen, 2006). Same measurements were reiterated for well-mixed scenarios with the two fans 'g_1' and 'g_2' on. The chamber was sterilized before and after each measurement by 75% ethanol and a 30-min ultraviolet light irradiation. Air samples collected for airborne bacteria counts were used to examine the chamber cleanliness.

2.2 Mathematical model

The airflow characteristics and deposition of microorganisms in the chamber without the mixing fans operating were investigated numerically. An enclosure with dimensions of 0.65 m (L) × 0.38 m (W) × 0.284 m (H) was modeled (Figure 1). Particles were injected continuously through the inlet. All of the airflow parameters chosen were based on the experimental values. Air was taken as 23ºC under isothermal conditions and five different inlet velocities namely 0.17 ms^{-1}, 0.58 ms^{-1}, 1.0 ms^{-1}, 1.4 ms^{-1} and 1.8 ms^{-1} were simulated. As the deposition of microorganisms is a very slow process (details below), the airflow and particle motion were modeled under steady-state conditions. One important input parameter is the particle shape which affects the particle motion; it was assumed spherical with a diameter of 1 μm. Because densities of the reference bacteria were not available in the literature, parametric sensitivity analysis allowing a range of densities from 1.0 g cm^{-3} to 1.3 g cm^{-3} was adopted for better assessment of how particle density could affect both the numerical and experimental results.

An Eulerian-Lagrangian approach was used to resolve the two-phase problem. The airflow issue was answered in an Eulerian framework while the transport and deposition of microorganisms were realized in a Lagrangian framework. Governing equations for the airflow and the discrete phase were solved by a commercial finite volume based CFD code FLUENT (version 6.3) with a second-order solution scheme for the airflow. The renormalization group (RNG) k-ε turbulence model, which has been applied successfully to shape various indoor environments (Chao et al. 2008; Qian et al. 2009; Lai and Cheng 2007), was taken up to simulate the airflow for the present environment. To couple the pressure and velocity fields, the PISO algorithm was employed. The grid convergence test was conducted with three mesh sizes by examining a set of airflow simulations. The three grid systems were 160 k, 320 k and 640 k. The

mean velocity for a horizontal line along the inlet and outlet was compared. Minor differences in the calculated results was observed between the coarsest and the other two finer grids. To further analysis the convergence of the three grids, the grid convergence index (GCI) proposed by Roache (1998) was adapted to determine the relative error of the air velocity magnitude at 100 points. GCI was calculated as,

$$GCI(u) = F_s \frac{\varepsilon_{rms}}{r^p - 1} \quad \ldots (1)$$

where u represents the velocity, the safety factor, $F_s = 3$ and $p = 2$. ε_{rms} is defined as,

$$\varepsilon_{rms} = \sqrt{\frac{\sum_{i=1}^{100} \left| (u_{coarse} - u_{fine}) / u_{fine} \right|^2}{100}} \quad \ldots (2)$$

r can be estimated by the following expression,

$$r = \left(\frac{N_{fine}}{N_{coarse}} \right)^{1/3} \quad \ldots (3)$$

where N is the number of grid.

Using the 160 k grid system as the reference, the GUI for the grid 320 k and 640 k are 4.9% and 4.2% respectively. Since the GUI values are all less than 5%, it indicates that the grids are sufficient fine. Considering both the computational time and accuracy, 320 k grid system was used in the simulations of this study and it is shown in Figure 3.

<< Figure 3: Mesh configuration of CFD prediction >>

The microorganism concentrations measured in the chamber were low (≤5,500 CFU m^{-3}). For a low volume fraction of the dispersed second phase, we can assume the effect of

particles on the turbulent flow is negligible. This one-way coupling allows the turbulence modulation effects to be neglected.

Lagrangian scheme was used to model the transport of the discrete phase. Each particle released from the injection site was tracked separately for its position, velocity and residence time. Due to the low bacteria concentration recorded in the experimental chamber, coagulation was also ignored. It was observed that the bacteria grew individually in the culture medium.

The equation of motion of a small aerosol particle which is calculated by integrating the force balance on the particle in terms of drag, gravity and Brownian forces can be written as,

$$\frac{du_p}{dt} = F_D(u - u_p) + \frac{g(\rho_p - \rho)}{\rho_p} + F_{\text{Brownian}} \quad \ldots (4)$$

where u_p and u are the particle and fluid parcel velocities, ρ_p and ρ are the particle (bacteria) and carrier phase densities, respectively.

$F_D(u_p - u)$ is the drag force per unit particle mass and F_D is defined as,

$$F_D = \frac{18\nu}{d_p^2 \rho} \frac{C_D \mathrm{Re}_p}{24} \quad \ldots (5)$$

where ν is the kinematic viscosity of the carrier phase, d_p is the particle diameter, and $\mathrm{Re_p}$ the particle Reynolds number is,

$$\mathrm{Re}_p = \frac{\rho_p d_p \left| u_p - u \right|}{\mu} \quad \ldots (6)$$

The drag coefficient C_D for a spherical particle is defined as,

$$C_D = a_1 + \frac{a_2}{\mathrm{Re}} + \frac{a_3}{\mathrm{Re}^2} \quad \ldots (7)$$

where a_1, a_2 and a_3 are the constants given by Morsi and Alexander (1972).

In some scenarios, the airflow rates were low and Brownian force affected the particle motion. For each time step, the amplitude of the Brownian force is expressed by (Li and Ahmadi 1992),

$$F_{\text{Brownian}} = \varsigma_i \sqrt{\frac{\pi S_o}{\Delta t}} \quad \ldots (8)$$

where $S_o = \dfrac{216\nu k_B T}{\rho d_p^5 (\rho_p / \rho)^2 C_c}$, ξ_i are zero-mean, unit-variance-independent Gaussian random numbers, Δt is the time step, T is the absolute temperature of the fluid, k_B is the Boltzmann constant, and C_c is the Cunningham slip correction respectively. Instantaneous particle velocity was determined by the discrete random walk model (DRW) which assumes the fluctuation velocities follows a Gaussian probability distribution as follows,

$$u_i^{'} = G\sqrt{\overline{u_i^2}} \quad \ldots (9)$$

where G is a zero mean, unit variance normally distributed random number, $\sqrt{\overline{u_i^2}}$ is the root mean square (RMS) local fluctuation velocity in the ith direction. For this model, it also assumes successive encounter of particles with discrete turbulence eddies and the eddy interaction time scale can be found elsewhere (FLUENT, 2006)

A reasonable and very common assumption was made for such a low velocity indoor airflow: once the particles touched a surface, they were considered 'trapped' and would not resuspend. To better understand the spatial deposition inside the chamber statistically, three different particle counts were tested, viz 2,000, 5,750 and 17,250. In some limited cases, 51,250

particles were injected. A sensitive analysis shown that 17,250 injection is a good choice as further increase of particle injection has insignificant influence of the simulation results on deposition. The objective was to investigate non-homogeneous distribution of bacteria deposition in an indoor environment. The floor of the enclosure was divided into seven equal sections along the length; depositions on the whole floor as well as within the sections were computed and saved to a file to be further analyzed and compared.

3. RESULTS AND DISCUSSIONS

3.1 Experimental results

Steady-state concentrations of the reference bacteria inside the ventilated chamber were examined. Their variations as found in five trial operations (each lasted 3 hours) were from 3% to 6% (with an exception of +15%). No significant concentration trend was observed during the sampling periods of all trials ($p \geq 0.3$, t-test). Furthermore, all deviations of temperature and relative humidity recorded in the center and corners of the chamber showed insignificant differences (≤ 0.2°C and ≤ 3% respectively) and would be normally distributed ($p \geq 0.3$, Shapiro-Wilk test). Hence, isothermal conditions were assumed throughout the trials.

The fractional bacteria counts C_{ij} represented the deposition distributions in the chamber. Assuming that each colony formed on the TSA plates was developed from one bacterial cell, C_{ij} measured on the plates for all of the 20 test conditions (i.e. 5 ventilation rates V_R, 2 reference bacteria, and 2 air mixing scenarios) as depicted in Figure 4 were given by the following equation, where Φ_{ij} is the total bacteria counts at location ij, i=1…7 and j=1…4 are the array coordinates of the TSA plates corresponding to the chamber fractional length x/L=0.069, 0.208,

0.346, 0.485, 0.623, 0.762, 0.9 and the chamber fractional width y/W=0.125, 0.375, 0.625, 0.875 respectively.

$$C_{ij} = \frac{\Phi_{ij}}{\sum_i \sum_j \Phi_{ij}} \quad \ldots (10)$$

<< Figure 4: Measured fractional bacteria counts on TSA plate array (i,j)=7×4 on the test chamber floor >>

It is noted for the values shown in Figure 4 are average values from repeated experiments of 2-4 times. It is also noted that the maximum and minimum values of each average case are not significantly different from the corresponding average value ($p \geq 0.3$, t-test). Figures 4(a) and 4(b) exhibit the spatial distributions of the fractional bacteria counts with the mixing fans on at V_R=1.7 h^{-1}, 6 h^{-1}, 10.3 h^{-1}, 14.5 h^{-1} and 18.8 h^{-1}; Figures 4(c) and 4(d) are those with the fans off. Preliminary visual inspections indicated that relatively uniform distributions in the chamber could be achieved via air mixing. Higher fractional bacteria counts were observed close to the outlet on plates i=6 and 7 in a number of ventilation rates with the mixing fans off.

Each test condition was repeated with N trials. The uniformity of the longitudinal spatial distributions can be described by the fractional bacteria counts C_i along x/L at i as displayed in Table 1. With an expected fractional count C_e=1/7, C_i were computed by,

$$C_i = \frac{\sum_j \Phi_{ij}}{\sum_i \sum_j \Phi_{ij}} \quad \ldots (11)$$

<< Table 1: Experimental results >>

Graphed in Figure 5 are the results of C_i against x/L. Pattern of C_i was assumed normally distributed ($p \geq 0.1$, Chi-square test). Error bars shown for one standard error of the average C_i. When the mixing fans were operating, the longitudinal distribution patterns of C_i found in all test conditions, except for rate (1) in case (a) as well as rates (4) and (5) in case (b), were uniform ($p \geq 0.05$, Chi-square test). When the mixing fans were not operating, all test conditions apart from rate (1) in case (d) gave non-uniform longitudinal distribution patterns of C_i ($p \leq 0.0005$, Chi-square test).

<< Figure 5: Fractional bacteria counts along the test chamber fractional length; (a)&(b) >>

In cases 5(c) and 5(d), despite there were some noted differences for the distribution patterns of *Micrococcus* at ventilation rates 6.0 h^{-1} and 18.8 h^{-1} ($p=0.06$, Chi-square test), the longitudinal distribution patterns of C_i were not significantly different among all ventilation rates ($p>0.2$, Chi-square test). Although the longitudinal fractional bacteria counts on plates $i=4$ (i.e. at $x/L=0.485$) were not significantly lower than the expected counts ($p \geq 0.25$, t-test), those on plates $i=1 \ldots 3$ (i.e. at $x/L \leq 0.346$) were ($p<0.1$, t-test). The total longitudinal fractional bacteria counts at $i=1 \ldots 3$ were also significantly lower than those at $i=5 \ldots 7$ ($p<0.0001$, t-test). In other words, both 5(c) and 5(d) showed a significant increasing trend ($p \leq 0.01$, t-test); and that can be expressed as a deposition ratio $\omega>1$ give by,

$$\omega = \frac{\sum_{i=5}^{7} C_i}{\sum_{i=1}^{3} C_i} \qquad \ldots (12)$$

The deposition ratios ω presented in Table 1 for cases 5(a) and 5(b) were not significantly larger than 1 ($p \geq 0.1$, t-test) whereas for cases 5(c) and 5(d) they were ($p \leq 0.005$, t-test). These

figures revealed that more bacteria were deposited in the floor section near the chamber wall opposite to the air inlet when air mixing was not enhanced by the mixing fans. The findings confirmed those reported by Bouilly et al. (2005).

It can be seen in Figure 6 that the deposition ratio ω is directly proportional to the ventilation rate. The correlations for both air mixing scenarios were significant ($R \geq 0.91$, $p < 0.05$, t-test). As the bioaerosols selected in this study were in the size range 0.7-1.8 μm, their movements were strongly influenced by the airflow pattern. It was noted that the higher the inlet velocity (or the ventilation rate), the higher was the air jet momentum (Chow and Wong 1998c). Increased deposition was due to increased particle collisions with the chamber walls (Kanaani et al. 2008b).

<< Figure 6: Deposition ratios >>

When the mixing fans were off during the tests, the average deposition ratios ranged from 1.10 to 1.89; on average 0.3 times of the average ratios obtained from those tests where the fans were on (i.e. ranged from 0.98 to 1.40). This difference reflected enhanced air mixing in the test chamber by operating the fans. In spite of the fact that air jet momentum would be slightly affected by the fan operation, the slopes of the two regression lines in Figure 6 were not significantly different ($p > 0.05$, t-test).

3.2 Modeled results

Velocity contours in the mid-plane x-z are shown in Figure 7. These profiles do not exhibit significant differences due to the simple inlet/outlet alignment through which inlet air travels to the outlet without creating a complex flow structure. For inlet velocities 0.17 ms^{-1} and 0.58 ms^{-1}, no observable eddies were detected (Figures 7 (a) and (b)). However, there were

visible eddies with higher inlet velocities. The vortex velocity was found to increase with the inlet airflow rate (Figures 7 (d) and (e)). Figures 8(a) and (b) shows the typical particle trajectories for velocity 0.17 ms^{-1} and 1.8 ms^{-1}. It can be observed that the particle motion follows closely to the air streamline lines in different velocities.

<< Figures 7(a) to (e): Velocity contours >>

<< Figures 8(a) & (b): Simulated particle trajectories >>

The percentage of the particles that escaped through the outlet without being mixed inside the chamber was determined. Regardless of the particle density selected, the outcome was in the range of 10-14%. Roughly 82 to 86% of the injected particles deposited inside the chamber. This low escape percentage can be attributed to the jet flow pattern. As expected, the smaller the percentage, the higher the airflow rate.

Table 2 summarizes the particle tracking results. Based on Table 2, a data file of where the particles were trapped on the floor was produced and processed. First of all, the total number of particles deposited onto the floor was counted. By setting up different boundary constraints, particles deposited in the defined longitudinal floor sections $\frac{1}{7}\mathrm{L},\frac{2}{7}\mathrm{L}, \ldots,\frac{7}{7}\mathrm{L}$ were then counted as Φ_1, Φ_2, …, Φ_7 respectively. Using $C_i = \frac{\Phi_i}{\sum_{i=1}^{7}\Phi_i}$, the fractional depositions listed in Table 2 were calculated and compared with the experimental results. As illustrated in Figure 9, the two results agreed quite well, especially in the inlet and center regions. Influences of the density range chosen for computation on the discrepancies of fractional bacteria counts were reported insignificant as shown in the figure ($p \geq 0.9$, Chi-square test). Aside from some discrepancies reported at 1.7 h^{-1} and 14.5 h^{-1} ($p=0.04$-0.06, Chi-square test), both results indicated that the

fractional bacteria count distributions were not significantly different among the test ventilation rates in between 1.7 h^{-1} and 18.8 h^{-1} ($p>0.1$, Chi-square test).

<< Table 2: Modeled results >>

The predicted deposition ratios were from 2.2 to 3.6, approximately 2 to 3 times the experimental values which were from 1.3 to 1.6. This disparity may be attributed to the counting of the bioaerosols and repeatability level of experiments. Depositions were measured on circular TSA plates in the experiments whereas they were predicted within rectangular floor sections in the mathematical model. The latter would overestimate the ratio. Moreover, the model did not take the plate heights, a 'very likely' barrier that would obstruct airflow around the floor, into account.

<< Figure 9: Fractional bacteria counts along the test chamber fractional length at ventilation rates from 1.7 h^{-1} to 18.8 h^{-1} >>

4. CONCLUSIONS

Multiple depositions of two microorganisms *Staphylococcus* and *Micrococcus* inside a test chamber were investigated under two air mixing conditions. Airflow rate was demonstrated to have an influence on the concentration homogeneity. The experimental results revealed that a small cooling fan inside the chamber prompted very effective mixing while non-homogeneity was observed even at a very high ventilation rate. The implication is significant that the ventilation rate and mixing conditions have influence on the bioaerosol dispersion and deposition in a test chamber. It is noted the present work would be limited in spherical species in the size of

choice. In the future, further work will be conducted to examine the depositions of microorganisms in spherical and non-spherical particle sizes other than 1 μm.

5. ACKNOWLEDGMENT

The work described in this paper was partially supported by grants from The Hong Kong Polytechnic University (Project account numbers G-SA04 and G-YG51) and the City University of Hong Kong (Project number 7002273).

REFERENCES

Bouilly, J., Limam, K., Béghein, C., and Allard, F. (2005). Effect on ventilation strategies on particle decay rates indoors: an experimental and modeling study, *Atmospheric Environment* 39:4885-4892.

Chao, C.Y.H., Wan, M.P., and Sze To, G.N. (2008). Transport and removal of expiratory droplets in hospital ward environment, *Aerosol Science and Technology* 42:377–394.

Chen, F.Z., Yu, S.C.M., and Lai, A.C.K. (2006). Modeling particle distribution and deposition in indoor environments with a new drift–flux model, *Atmospheric Environment* 40:357–367.

Chow, W.K., and Wong, L.T. (1994). Experimental studies on air diffusion of a linear diffuser and associated thermal comfort indices in an air-conditioned space, *Building and Environment* 29:523-530.

Chow, W.K., and Wong, L.T. (1998a). Equations for a ventilation design derived from computational fluid dynamics, *Indoor and Built Environment* 7:276-288.

Chow, W.K., and Wong, L.T. (1998b). Survey on the air diffusion devices for air-conditioning systems in Hong Kong, *Energy Engineering* 95(6):50-79.

Chow, W.K., and Wong, L.T. (1998c). Air diffusion terminal devices: macroscopic numbers describing jet momentum, *Building Services Engineering Research and Technology* 19:49-54.

Fanger, P.O., Melikov, A.K., Hanzawa, H., and Ring, J. (1988). Air turbulence and sensation of draught, *Energy and Buildings* 12:21-39.

FLUENT (2006). FLUENT 6.3 User's Guide. Fluent Inc, Lebanon.

Gandara, A., Mota, L.C., Flores, C., Perez, H.R., Green, C.F., Gibbs, S.G. (2006). Isolation of *Staphylococcus aureus* and anitbiotic-resistant *Staphylococcus aureus* from residential indoor bioaerosols, *Environmental Health Perspectives* 114:1859–1864.

Gao, N.P., and Niu, J.L. (2007). Modeling particle dispersion and deposition in indoor environments, *Atmospheric Environment* 41:3862–3876.

Górny, R.L., and Dutkiewicz, J. (2002). Bacterial and fungal aerosols in indoor environment in Central and Eastern European countries, *Annals of Agricultural and Environmental Medicine* 9:17–23.

Holt, J.G., Krieg, N.R., Sneath, P.H.A., Staley, J.T., and Williams, S.T. (1994). *Bergey's manual® of determinative bacteriology (9th Ed.)* Williams & Wilkins, Baltimore, USA.

ISO (1994). ISO 10648-2:1994(E). Containment enclosures – Part 2: Classification according to leak tightness and associated checking methods. International Standard.

Kanaani, H., Hargreaves, M., Ristovski, Z., and Morawska, L. (2008a). Deposition rates of fungal spores in indoor environments, factors effecting them and comparison with non-biological aerosols, *Atmospheric Environment* 42:7141–7154.

Kanaani, H., Hargreaves, M., Smith, J., Ristovski, Z., Agranovski, V., Morawska, L. (2008b). Performance of UVAPS with respect to detection of airborne fungi, *Journal of Aerosol Science* 39:175–189.

Lai, A.C.K. (2002). Particle deposition indoors: A review, *Indoor Air* 12:211–214.

Lai, A.C.K., and Cheng, Y.C. (2007). Study of expiratory droplet dispersion and transport using a new Eulerian modeling approach, *Atmospheric Environment* 41:7473–7484.

Lai, A.C.K., Chen, F.Z. (2006). Modeling particle deposition and distribution in a chamber with two-equation Reynolds-averaged Navier-Stokes model, *Journal of Aerosol Science* 37: 1770-1780.

Lai, A.C.K., Mui, K.W., Wong, L.T. and Law, L.Y. (2009). An evaluation model for indoor environmental quality (IEQ) acceptance in residential buildings, *Energy and Buildings*, In press. doi:10.1016/j.enbuild.2009.03.016

Li, A. and Ahmadi, G. (1992). Dispersion and Deposition of Spherical Particles from Point Sources in a Turbulent Channel Flow, *Aerosol Science and Technology* 16:209-226.

Li, Y., Leung, G.M., Tang, J.W., Yang, X., Chao, C.Y.H., Lin, J.Z., Lu, J.W., Nielsen, P.V., Niu, J., Qian, H., Sleigh, A.C., Su, H.-J.J., Sundell, J., Wong, T.W., and Yuen, P.L. (2007). Role of ventilation in airborne transmission of infectious agents in the built environment — a multidisciplinary systematic review, *Indoor Air* 17:2–18.

Morsi, S. A., and Alexander, A. J. (1972). An investigation of particle trajectories in two-phase flow systems, *Journal of Fluid Mechanics* 55:193-208.

Mui, K.W., Wong, L.T., Wu, C.L., and Lai, A.C.K (2009). Numerical modeling of exhaled droplet nuclei dispersion and mixing in indoor environments, *Journal of Hazardous Materials* 167:736-744.

Nazaroff, W.W. (2004). Indoor particle dynamics., *Indoor Air* 14(S7):175-183.

Otten, J.A., and Burge, H.A. (1999). Bacteria. In Macher JM, Ammann HM, Burge HA, Milton DK, Morey PM (eds.) Bioaerosols: Assessment and Control, Cincinnati, OH, American Conference of Governmental Industrial Hygienists, p.18-1–18-10.

Qian, H., Li, Y., Nielsen P.V., and Huang, X. (2009). Spatial distribution of infection risk of SARS transmission in a hospital ward, *Building and Environment* 44:1651-1658.

Roache, P.J. (1998). Verification of codes and calculation, *AIAA Journal* 36:696-702.

Sandberg, M., and Sjoberg, M. (1983). The use of moments for assessing air quality in ventilated rooms. *Building and Environment* 18:181-197.

Stanley, J.T. (1989). *Bergey's manual of systematic bacteriology*. 1st Ed. Williams & Wilkins, Baltimore.

Tsai, F.C., and Macher, J.M. (2005). Concentrations of airborne culturable bacteria in 100 large US buildings from the BASE study, *Indoor air* 15(S9):71–81.

Toivola, M., Alm, S., Reponen, T., Kolari, S., and Nevalainen, A. (2002). Personal exposures and microenvironmental concentrations of particles and bioaerosols. *Journal of Environmental Monitoring* 4: 166-174.

Wan, M.P., and Chao, C.Y.H. (2007). Transport characteristics of expiratory droplets and droplet nuclei in indoor environments with different ventilation airflow patterns, *J. Biomech. Eng. Trans. ASME* 129:341–353.

Wong, L.T., Mui, K.W., and Hui, P.S. (2006). A statistical model for characterizing common air pollutants in air-conditioned offices, *Atmospheric Environment* 40:4246-4257.

Zhao, B., Zhang, Z., and Li, X. (2005). Numerical study of the transport of droplets or particles generated by respiratory system indoors, *Building and Environment* 40:1032–1039.

LIST OF FIGURES AND TABLES

Table 1: Experimental results

Table 2: Modeled results

Table 1: Experimental results

Case	Ventilation rate V_R (h^{-1})	Trials N	Fractional counts C_i on TSA plate i at a fractional distance x/L from the inlet							Deposition ratio ω
			i=1	2	3	4	5	6	7	
			x/L=0.069	0.208	0.346	0.485	0.623	0.762	0.900	
Scenario (1): With mixing fans										
(a) Staphylococcus	(1) 1.7	3	0.165	0.141	0.133	0.130	0.120	0.131	0.179	0.98
	(2) 6.0	4	0.141	0.144	0.136	0.139	0.142	0.153	0.145	1.04
	(3) 10.3	3	0.121	0.144	0.142	0.136	0.153	0.155	0.149	1.12
	(4) 14.5	4	0.133	0.143	0.139	0.142	0.149	0.146	0.147	1.06
	(5) 18.8	3	0.120	0.123	0.139	0.155	0.178	0.153	0.131	1.21
(b) Micrococcus	(1) 1.7	3	0.138	0.136	0.145	0.141	0.149	0.143	0.147	1.05
	(2) 6.0	4	0.111	0.124	0.148	0.150	0.155	0.148	0.164	1.22
	(3) 10.3	3	0.118	0.150	0.152	0.139	0.148	0.144	0.150	1.05
	(4) 14.5	4	0.092	0.122	0.160	0.144	0.159	0.156	0.166	1.28
	(5) 18.8	3	0.109	0.131	0.119	0.139	0.201	0.160	0.141	1.40
Scenario (2): Without mixing fans										
(c) Staphylococcus	(1) 1.7	2	0.131	0.115	0.115	0.132	0.138	0.167	0.201	1.40
	(2) 6.0	3	0.104	0.098	0.143	0.165	0.171	0.157	0.163	1.42
	(3) 10.3	3	0.105	0.113	0.127	0.145	0.154	0.168	0.188	1.48
	(4) 14.5	3	0.103	0.107	0.124	0.152	0.162	0.170	0.182	1.54
	(5) 18.8	3	0.104	0.097	0.100	0.129	0.183	0.182	0.204	1.89
(d) Micrococcus	(1) 1.7	3	0.139	0.133	0.128	0.159	0.139	0.143	0.160	1.10
	(2) 6.0	2	0.147	0.104	0.120	0.121	0.139	0.139	0.231	1.37
	(3) 10.3	2	0.099	0.107	0.143	0.161	0.164	0.167	0.159	1.41
	(4) 14.5	2	0.120	0.106	0.127	0.156	0.211	0.122	0.158	1.39
	(5) 18.8	2	0.096	0.105	0.141	0.190	0.172	0.168	0.129	1.37

Table 2: Modeled results

Ventilation rate V_R (h^{-1})	1.7			5.6			10.4			14.6			18.6		
Density (g cm^{-3})	**1.0**	**1.1**	**1.3**	**1.0**	**1.1**	**1.3**	**1.0**	**1.1**	**1.3**	**1.0**	**1.1**	**1.3**	**1.0**	**1.1**	**1.3**
Fractional escape	0.1322	0.1343	0.1336	0.1270	0.1264	0.1243	0.1199	0.1219	0.1216	0.1164	0.1153	0.1168	0.1131	0.1134	0.1106
Fractional deposition	0.8663	0.8642	0.8660	0.8724	0.8730	0.8748	0.8797	0.8775	0.8781	0.8833	0.8840	0.8826	0.8866	0.8861	0.8890
x/L	**Fractional deposition at x/L**														
0.93	0.1432	0.1446	0.1408	0.2284	0.2275	0.2298	0.2402	0.2440	0.2442	0.2588	0.2567	0.2513	0.2507	0.2409	0.2464
0.79	0.2277	0.2268	0.2220	0.2351	0.2360	0.2343	0.2294	0.2283	0.2316	0.2486	0.2396	0.2431	0.2381	0.2456	0.2328
0.64	0.2006	0.2065	0.1985	0.1783	0.1791	0.1824	0.1656	0.1670	0.1635	0.1729	0.1802	0.1768	0.1713	0.1727	0.1657
0.50	0.1681	0.1651	0.1726	0.1422	0.1392	0.1389	0.1366	0.1403	0.1377	0.1375	0.1385	0.1417	0.1477	0.1495	0.1551
0.36	0.1266	0.1192	0.1249	0.1001	0.0981	0.0982	0.1038	0.1006	0.1027	0.0819	0.0840	0.0832	0.0949	0.0895	0.0948
0.21	0.0845	0.0845	0.0846	0.0689	0.0726	0.0687	0.0774	0.0718	0.0748	0.0503	0.0493	0.0534	0.0538	0.0537	0.0538
0.07	0.0493	0.0533	0.0566	0.0469	0.0477	0.0477	0.0470	0.0480	0.0455	0.0500	0.0517	0.0505	0.0434	0.0480	0.0515

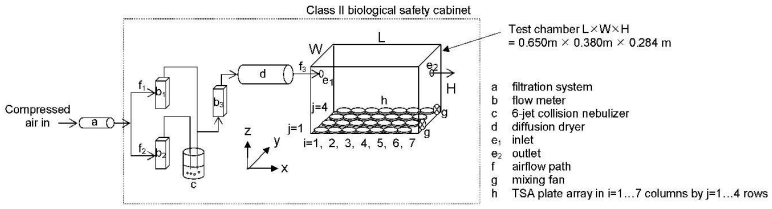

297x209mm (300 x 300 DPI)

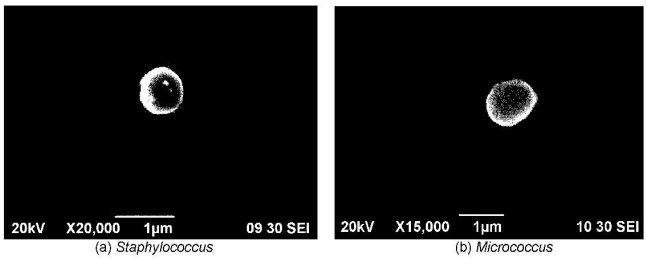

(a) *Staphylococcus* (b) *Micrococcus*

297x209mm (300 x 300 DPI)

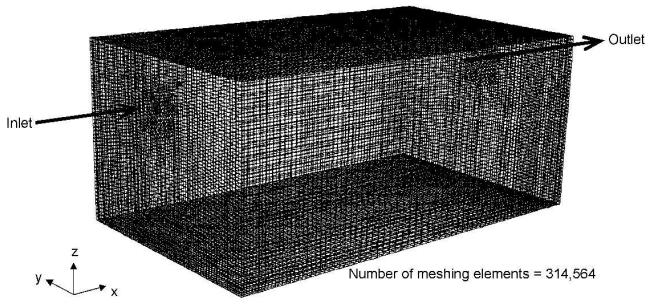

297x209mm (300 x 300 DPI)

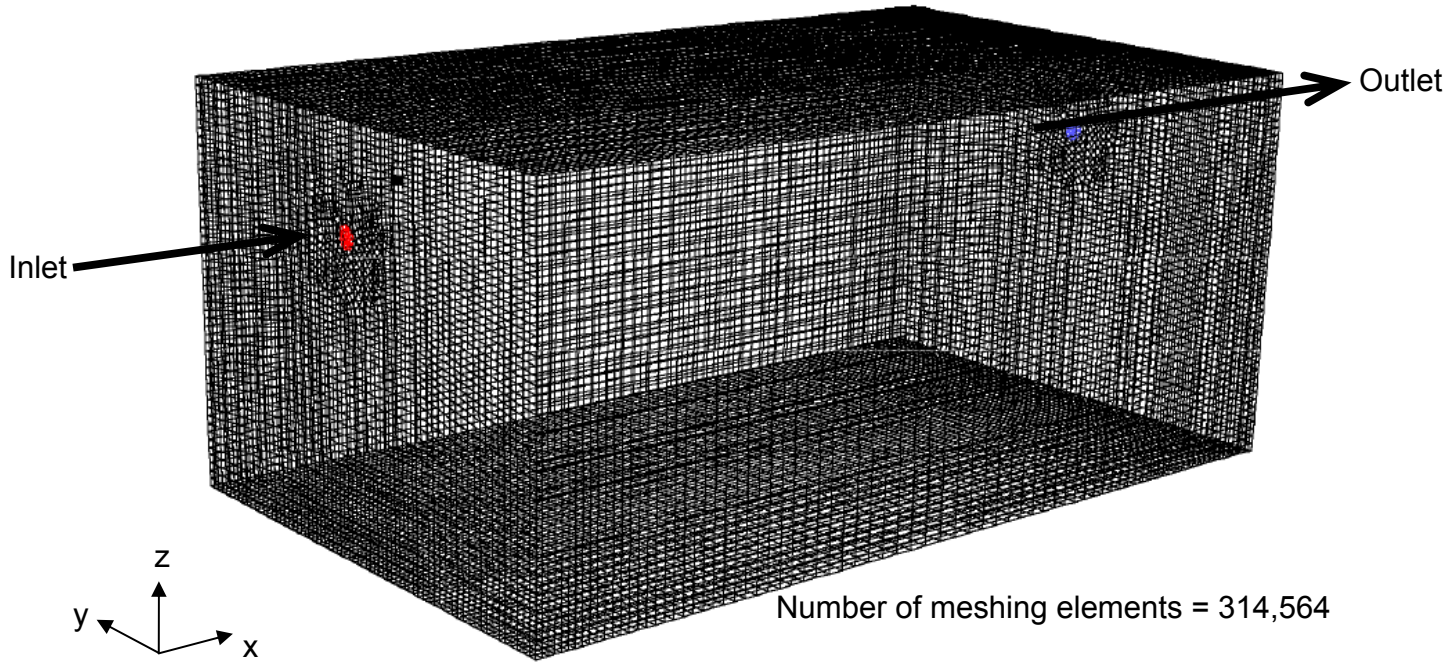
Outlet
Inlet
z
y
x
Number of meshing elements = 314,564

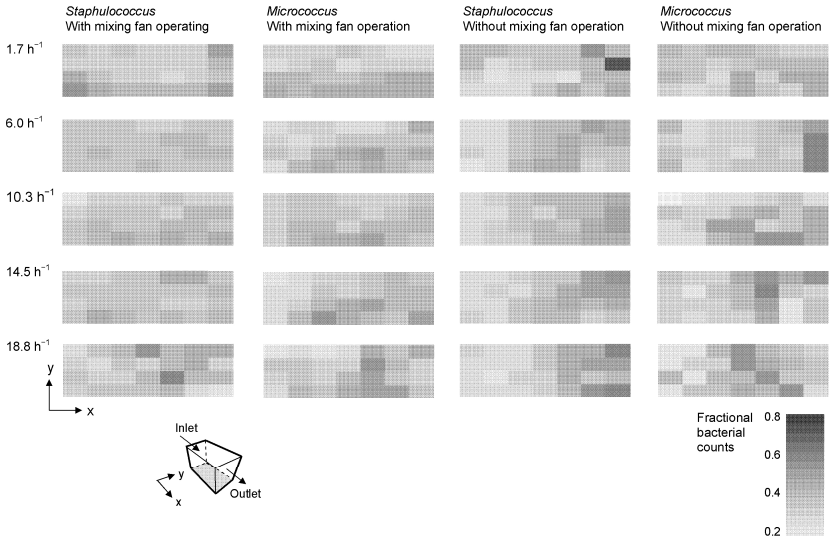

297x209mm (300 x 300 DPI)

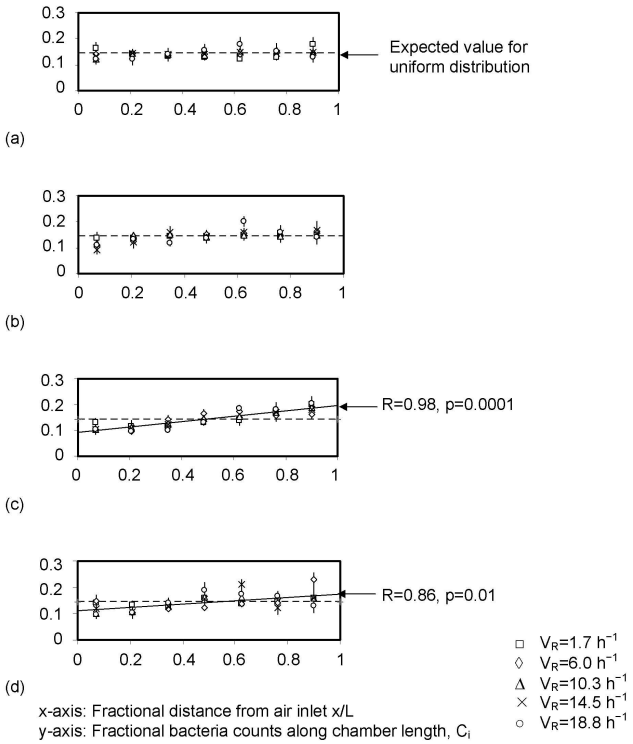

209x297mm (300 x 300 DPI)

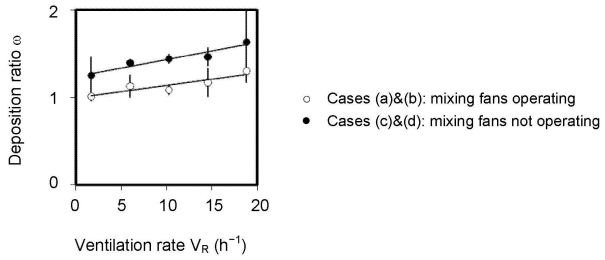

209x297mm (300 x 300 DPI)

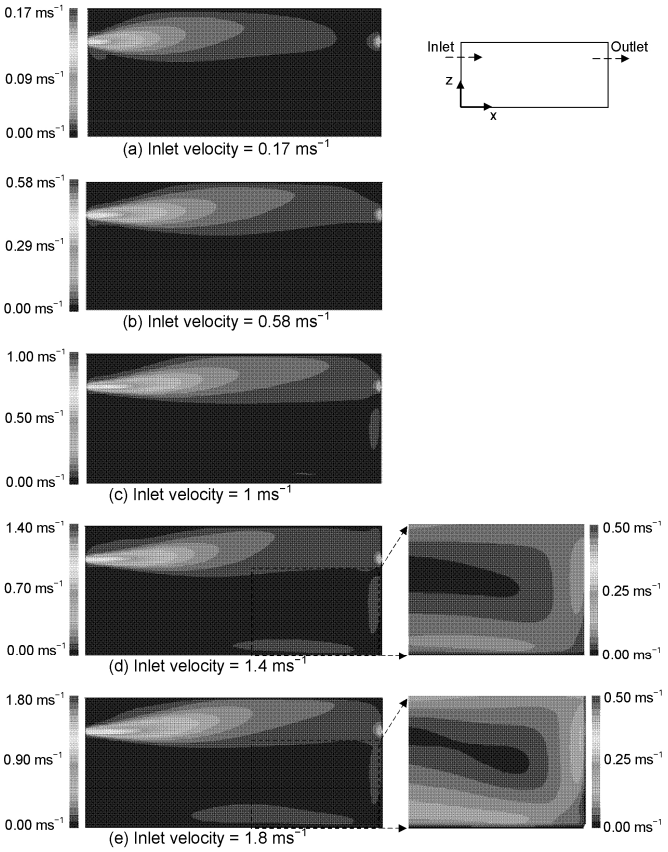

209x297mm (300 x 300 DPI)

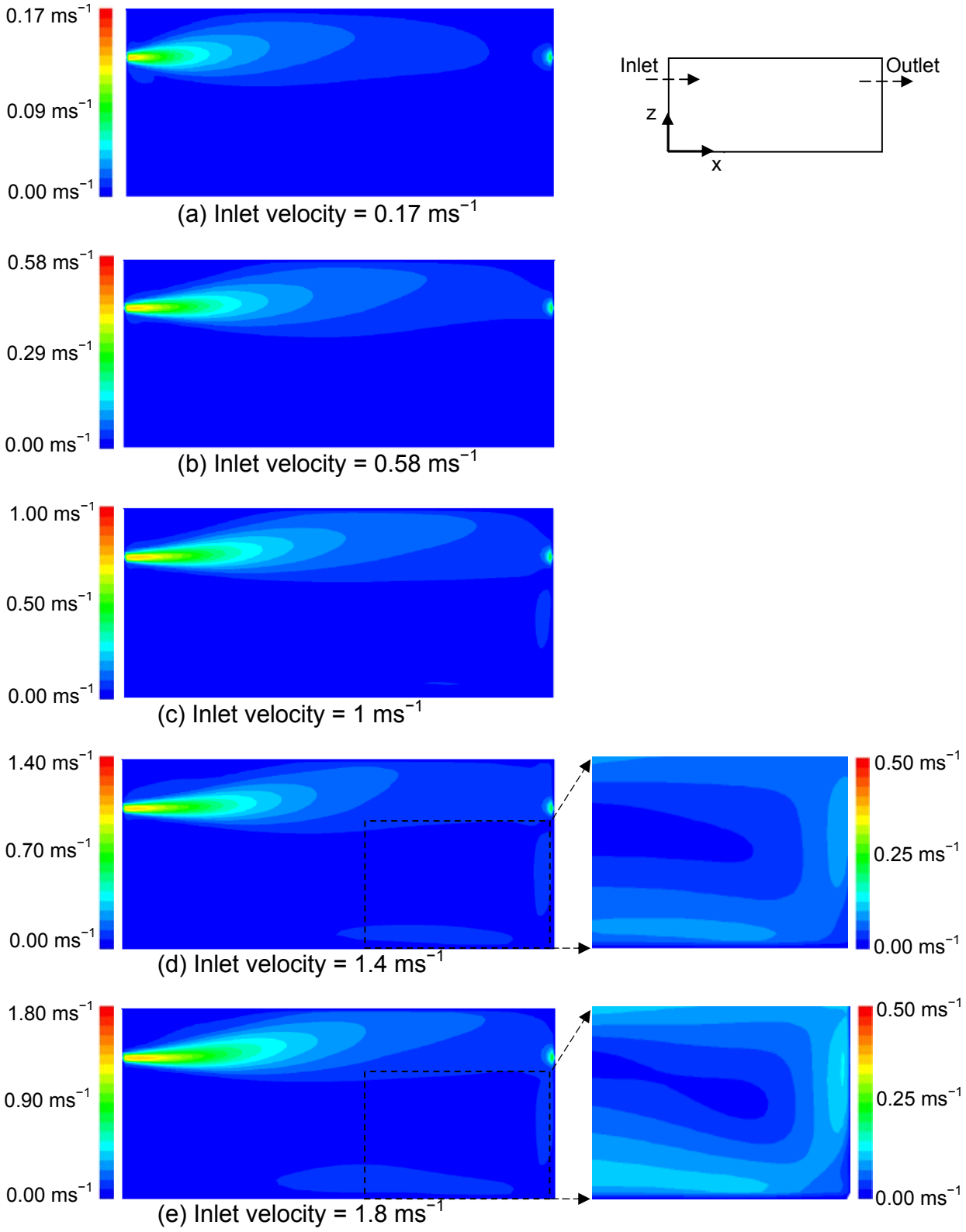
0.17 ms^{-1}
0.09 ms^{-1}
0.00 ms^{-1}
Inlet
Outlet
z
x
(a) Inlet velocity = 0.17 ms^{-1}
0.58 ms^{-1}
0.29 ms^{-1}
0.00 ms^{-1}
(b) Inlet velocity = 0.58 ms^{-1}
1.00 ms^{-1}
0.50 ms^{-1}
0.00 ms^{-1}
(c) Inlet velocity = 1 ms^{-1}
1.40 ms^{-1}
0.70 ms^{-1}
0.00 ms^{-1}
0.50 ms^{-1}
0.25 ms^{-1}
0.00 ms^{-1}
(d) Inlet velocity = 1.4 ms^{-1}
1.80 ms^{-1}
0.90 ms^{-1}
0.00 ms^{-1}
0.50 ms^{-1}
0.25 ms^{-1}
0.00 ms^{-1}
(e) Inlet velocity = 1.8 ms^{-1}

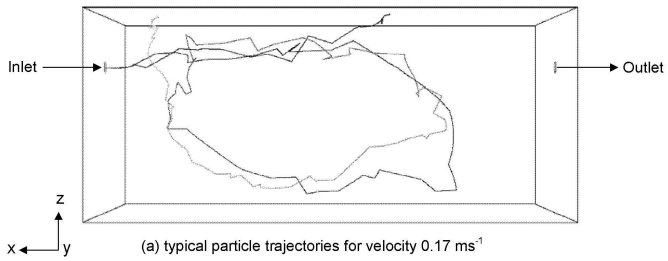

(a) typical particle trajectories for velocity 0.17 ms^{-1}

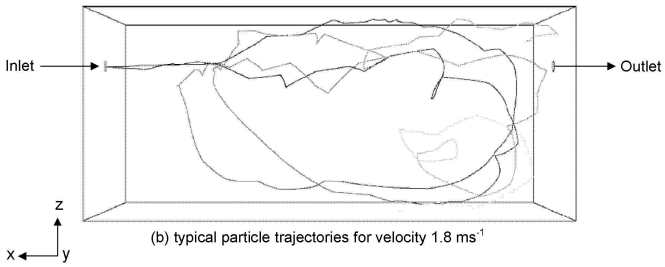

(b) typical particle trajectories for velocity 1.8 ms^{-1}

209x297mm (300 x 300 DPI)

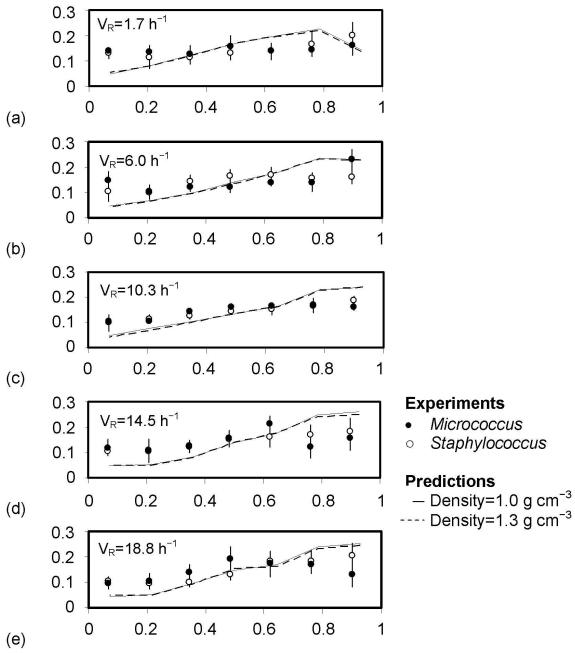

209x297mm (300 x 300 DPI)

AMERICAN ASSOCIATION FOR AEROSOL RESEARCH (AAAR) Copyright Transfer Agreement
AST-MS-2009-089.R2

Before this manuscript can be published, the following agreement must be signed by at least one author and returned to:
AAAR/AS&T Editorial Office
919 W. 53rd Street
Minneapolis, MN 55419
Phone: (612) 827-2421
FAX: (651) 925-0278

Article Title:
An experimental and numerical study on deposition of bioaerosols in a scaled chamber

by Wong, L.T.; Lai, Alvin C. K.; Chan, W.Y.; Mui, K.W.

1. The Author(s) hereby transfers to the American Association for Aerosol Research (AAAR) copyright to the above article*, subject to its acceptance by Aerosol Science and Technology (AST). This copyright includes all material in any media to be published as part of the Article now or in the future. AAAR shall have the exclusive and unlimited right to publish the Article during the full term of copyright including renewals and extensions and all subsidiary rights as indicated above subject to the exceptions in (3) below.

2. The Author(s) warrants that the work has not been published before, and is not under consideration for publication in any other journals. Furthermore, the Author(s) warrants that the article contains no matter that is libelous, obscene, or otherwise contrary to law.

3. The Author(s) may reproduce the Article by any means without fee or permission for not-for-profit educational or classroom purposes with the exception of reproduction by services that collect fees for delivery of documents. The copyright notice that appeared in the original published work must be included on all copies. The Author(s) may use part or all of this Article in any future works of his/her (their) own. When this is done, specific reference that this work was originally published in Aerosol Science & Technology must be included. The Author(s) retain the right to post a copy of the Article on the Author(s) web site after the article is published in AST and to translate and distribute translated copies of the article. In any reproduction, the original publication in AST must be credited in the following manner: "First published in Aerosol Science and Technology, Volume (Issue), Pages, Year." Web postings shall include a link to the online Abstract of the Article at the AST web site: www.AAAR.org/ASandT

4. AAAR retains the right to grant others use of figures or tables in reviews or other articles.

5. The Author(s) retains all proprietary rights other than copyright, such as patent rights.

This form is to be signed by the Author(s) or, in the case of a "work-made-for-hire," by the employer. If there is more than one Author, then either all must sign, or one Author may sign for all. In the latter case, the Author who signs must inform co-authors of the above terms.

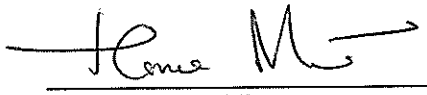

15 Oct 2009

Signature and Date

MUI Kwok-Wai, Assistant Professor
Print Name and Title

Dept. of Building Services Engineering, The Hong Kong Polytechnic University,
Institution Name

Room FJ713, Dept of BSE, The Hong Kong Polytechnic University,
Street Address

Hung Hom, Kowloon, Hong Kong
City State/Province

Hong Kong (HKSAR)
Postal Code and Country (if outside USA)

*U.S. Government Employees
A work prepared by U.S. Government officers or employees as a part of their official duties is not eligible for U.S. Copyright. If all the authors are in this category, one of the authors should sign below, and indicate his or her affiliation. If at least one author is not in this category, that author should sign the above copyright agreement.

_____ _____ Signature and Date

_____
Print Name and Title

_____
Department/Agency Name

_____
Street Address

_____
City State/Province

_____
Postal Code and Country (if outside USA)